



Global and regional variability in marine surface temperatures

Citation

Laepple, T., and P. Huybers. 2014. "Global and Regional Variability in Marine Surface Temperatures." *Geophysical Research Letters* 41 (7) (April 1): 2528–2534.
doi:10.1002/2014gl059345.

Published Version

doi:10.1002/2014gl059345

Permanent link

<http://nrs.harvard.edu/urn-3:HUL.InstRepos:25667322>

Terms of Use

This article was downloaded from Harvard University's DASH repository, and is made available under the terms and conditions applicable to Other Posted Material, as set forth at <http://nrs.harvard.edu/urn-3:HUL.InstRepos:dash.current.terms-of-use#LAA>

Share Your Story

The Harvard community has made this article openly available.
Please share how this access benefits you. [Submit a story](#).

[Accessibility](#)



RESEARCH LETTER

10.1002/2014GL059345

Key Points:

- Methods are introduced to compare instrumental and model SST variability
- Regional SST variability is underestimated by CMIP5 models at decadal timescales
- Lack of SST variability may explain the difficulty in simulating recent trends

Correspondence to:

T. Laepple,
thomas.laepple@awi.de

Citation:

Laepple, T., and P. Huybers (2014), Global and regional variability in marine surface temperatures, *Geophys. Res. Lett.*, *41*, 2528–2534, doi:10.1002/2014GL059345.

Received 20 JAN 2014

Accepted 7 MAR 2014

Accepted article online 13 MAR 2014

Published online 1 APR 2014

Global and regional variability in marine surface temperatures

T. Laepple¹ and P. Huybers²

¹ Alfred Wegener Institute, Helmholtz Centre for Polar and Marine Research, Potsdam, Germany, ²Earth and Planetary Sciences, Harvard University, Cambridge, Massachusetts, USA

Abstract The temperature variability simulated by climate models is generally consistent with that observed in instrumental records at the scale of global averages, but further insight can also be obtained from regional analysis of the marine temperature record. A protocol is developed for comparing model simulations to observations that account for observational noise and missing data. General consistency between Coupled Model Intercomparison Project Phase 5 model simulations and regional sea surface temperature variability is demonstrated at interannual timescales. At interdecadal timescales, however, the variability diagnosed from observations is significantly greater. Discrepancies are greatest at low latitudes, with none of the 41 models showing equal or greater interdecadal variability. The pattern of suppressed variability at longer timescales and smaller spatial scales appears consistent with models generally being too diffusive. Suppressed variability of low-latitude marine temperatures points to underestimation of intrinsic variability and may help explain why few models reproduce the observed temperature trends during the last 15 years.

1. Introduction

Accurate representation of the spread in predictions of future climate is, arguably, as important as correctly predicting a central value. Comparison against observed variability is one means of evaluating the skill of general circulation models (GCMs) in simulating the spread of plausible temperatures. At the global scale, the observed temperature variability is generally consistent with that produced by GCMs both in terms of overall magnitude and spectral distribution [Solomon *et al.*, 2007; Jones *et al.*, 2013]. Although regional model-data consistency has also generally been found at synoptic to interannual timescales [Collins *et al.*, 2001; Min *et al.*, 2005], discrepancies have been noted in regional variability at longer timescales. Stott and Tett [1998] found that simulations from a climate model underestimate surface temperature variability at scales less than 2000 km. Davey *et al.* [2002] and DelSole [2006] also suggested that collections of models underestimate regional low-frequency variability at decadal timescales relative to observations, and Santer *et al.* [2006] found a similar mismatch for eastern tropical Atlantic sea surface temperature (SST).

There are two classes of explanation for model-data discrepancies in regional SST variability. The first is for model simulations to inadequately simulate variability. The second class of explanation is for observational errors, data inhomogeneities, or interpolation artifacts to bias instrumental estimates of variability. These data issues were not systematically treated in foregoing studies, raising the question of whether discrepancies arise from model or data short-comings.

To address these possibilities we extend upon foregoing model-data comparison studies in three respects. First, analysis of the Coupled Model Intercomparison Project Phase 5 (CMIP5) archive [Taylor *et al.*, 2012] offers a more recent set of 163 historical simulations to compare against observations. Second, recently developed corrections for data inhomogeneities along with more complete estimates of uncertainty [Kennedy *et al.*, 2011a, 2011b] permit for more accurate assessment of observational variability. Finally, we introduce and apply a new technique to correct for the effects of data gaps upon variance and spectral estimates. Such accounting for variance contributions to the estimated SST variability permits for less biased model-data comparison.

2. Simulations and Data

For simulations we rely on the CMIP5 collection of coupled atmosphere-ocean model runs. Analysis is of the SST fields of historical simulations covering 1861–2005 (CMIP5) that are forced by reconstructed natural

and anthropogenic radiative forcing from solar variations, greenhouse gas concentrations, and volcanic and anthropogenic aerosols. In all, there are 163 simulations from 41 models. Simulations are placed onto the $5 \times 5^\circ$ grid of the HadSST3 data set by first interpolating to a uniform $0.25 \times 0.25^\circ$ grid and then averaging to $5 \times 5^\circ$ boxes. This high-resolution interpolation followed by averaging avoids spatial aliasing that would otherwise lead to biases in estimated variability. SST anomalies are then computed by removing the monthly climatology calculated between 1960 and 1990.

Instrumental observations are from the HADSST3 compilation of sea surface temperatures (SST) [Kennedy *et al.*, 2011a, 2011b]. This data set consists of binned SST observations from ships and buoys on a 5° by 5° grid, where averaging is conducted after excluding outliers. The time series are bias corrected for spurious trends caused by changes in measurement techniques but are not interpolated or variance adjusted, as is appropriate for our purposes. Uncertainty estimates associated with observational noise, binning, and bias correction are all provided [Kennedy *et al.*, 2011a, 2011b].

SST records are primarily from ship measurements that, outside of certain heavily trafficked routes, tend to contain observational gaps. Annual mean SST estimates are only computed when at least 10 observations are present within the year. Analyzed time series are the longest possible at each grid box for which no more than 10% of years are missing and for which data is present during the first and last years. Missing years are linearly interpolated for. The last year is always fixed at 2005 in order to overlap with the time span covered by the historical CMIP5 simulations. Further, as our focus is on multidecadal variations in SSTs, time series must cover at least 100 years after interpolation in order to be included.

To provide for an equivalent basis for model-data comparison, missing months in the observations are censored in the simulation results. Interpolation will typically alter spectral estimates [Wilson *et al.*, 2003; Rhines and Huybers, 2011], but because equivalent months and years are missing from both the simulations and observations, comparisons between the two are not biased, excepting for certain issues involving correcting for noise components in the observational data set that are addressed shortly.

3. Spectral Estimation and Noise Correction

Timescale-dependent variance is estimated in both the instrumental observations and model simulations by summing spectral energy estimates between frequencies of $1/2$ – $1/5$ years⁻¹ for interannual variations and $1/20$ – $1/50$ years⁻¹ for interdecadal variations. For the variance estimate, we sum across the relevant frequencies of a periodogram [e.g., Bloomfield, 1976], whereas the multitaper method with three windows [Percival and Walden, 1993] is used for visually presenting results. The periodogram is used for timescale-dependent variance estimates because the multitaper method is slightly biased at the lowest frequencies [McCoy *et al.*, 1998]. All spectral analyses are performed after linearly detrending the SST time series.

Instrumental SST records contain substantial noise, with the average monthly observation having a 1 standard-deviation uncertainty of 0.48°C [Kennedy *et al.*, 2011a]. Noise estimates are available for each month and grid box and are calculated taking into account random measurement errors, errors stemming from incomplete spatial coverage of the 5° by 5° grid box, and incomplete temporal coverage of the observed month. For regional variance estimates, we treat these sources of noise as independent between months because measurements from ships are unlikely to correlate in a single location over different months, and measurements from buoys have relatively small uncertainties (J. Kennedy, personal communication, 2012). For the global mean SST estimate, we use measurement and sampling error estimates that account for spatial and temporal correlations [Kennedy *et al.*, 2011a].

Independent realization of normally distributed noise is expected to have a uniform spectral distribution in the case of uniform sampling, but the presence of gaps in regional observational records leads to a variable noise influence with frequency. Essentially, interpolation between noisy values introduces autocorrelated noise. To correct for these noise contributions, we generate annually resolved time series from draws of a normal distribution having time variable standard deviation consistent with the reported error. Years with missing observations are linearly interpolated for, and the spectral estimate of the realized noise sequence is computed. This process is repeated 10,000 times, and the average across-noise spectra are calculated and removed from the corresponding instrumental SST spectral estimate. This technique shares some similarities with that introduced by Laepple and Huybers [2013] for correcting the spectral estimates associated with

Table 1. Variance Ratios of Instrumental and Simulated SSTs and Their Dependence on Correction Choices and Data Restriction Criteria^a

	Time Period	Data Restriction	Mid-High Latitudes > 30°S > 30°N		Tropics and Subtropics 30°S–30°N	
			2–5 years	20–50 years	2–5 years	20–50 years
Uncorrected	1861–2005	≥1 obs/yr	2.04 (1.85–2.23)	1.8 (1.33–2.34)	2.11 (1.92–2.31)	2.86 (2.11–3.72)
	1861–2005	≥10 obs/yr	1.44 (1.3–1.57)	1.43 (1.06–1.87)	1.63 (1.48–1.78)	2.24 (1.65–2.92)
	1900–2005	≥10 obs/yr	1.25 (1.12–1.39)	1.37 (0.97–1.83)	1.48 (1.32–1.65)	2.12 (1.51–2.84)
	1900–1960	≥10 obs/yr	1.39 (1.18–1.61)	1.31 (0.87–1.84)	1.6 (1.36–1.85)	2.64 (1.76–3.7)
	1961–2005	≥10 obs/yr	1.43 (1.21–1.68)	1.33 (0.81–1.98)	1.47 (1.24–1.73)	1.82 (1.11–2.7)
Corrected	1861–2005	≥1 obs/yr	1.19 (1.08–1.3)	1.55 (1.14–2.02)	1.02 (0.93–1.12)	2.19 (1.62–2.86)
	1861–2005	≥10 obs/yr	1.04 (0.94–1.14)	1.32 (0.98–1.72)	1.06 (0.97–1.16)	1.92 (1.42–2.51)
	1900–2005	≥10 obs/yr	0.99 (0.89–1.1)	1.3 (0.93–1.74)	1.09 (0.97–1.21)	1.93 (1.37–2.58)
	1900–1960	≥10 obs/yr	1.07 (0.91–1.24)	1.23 (0.82–1.72)	1.01 (0.86–1.17)	2.28 (1.52–3.2)
	1961–2005	≥10 obs/yr	0.98 (0.82–1.15)	1.19 (0.72–1.76)	1.08 (0.91–1.27)	1.51 (0.92–2.24)

^aNote that variance ratios are independent of the data restriction criteria after correction for noise sources, whereas the inclusion of sparsely sampled grid boxes otherwise leads to greater variance. 95% confidence intervals are calculated assuming 10 spatial degrees of freedom and 1 degree of freedom per model simulation.

paleoclimate records, and it is applied to the time series associated with each grid box included in the analysis. The correction for excess variance has the largest proportional effects at interannual timescales, rather than decadal ones, because spectral magnitudes are smaller at higher frequencies. The correction at the global level is more simple, having a uniform distribution across frequency, because there are no data gaps.

Prior to correction, the variance ratio between the observed and simulated temperatures has a cross correlation with the average number of observations per year across grid boxes of $r = -0.38$. This negative correlation is significant at the 95% confidence level, assuming at least 28 degrees of freedom and is expected on the basis of fewer observations leading to greater noise in the annual temperature estimates. After correction, the magnitude of the correlation is reduced to a value that is statistically indistinguishable from zero, $r = 0.03$, indicating that the correction is successful in removing excess noise. Also important is that, after correction, the variance ratio shows no dependence on what time interval is analyzed nor upon what data coverage criteria are applied for admitting annual temperature estimates (Table 1). Note that variance-adjusted products were provided in earlier versions of the HadSST data set but are not used here because HadSST variance adjustment is accomplished through exclusively rescaling the amplitude of high-frequency variability in order to homogenize variance differences expected from differences in the signal-to-noise ratios [Brohan et al., 2006]. We have no expectation for noise to be band limited and apply a correction across the entirety of spectrum that partially reduces model-data differences at low frequencies.

Uncertainties reported in Table 1 include those usually associated with finite data as well as the uncertainties associated with removal of the noise component. In addition, there also exist uncertainties in the instrumental SST data set stemming from corrections applied for systematic changes in measurement techniques [Kennedy et al., 2011b]. To account for these systematic uncertainties, we analyze the 100 available realizations of the HadSST3 field that seek to cover the range of instrumental biases and include the resulting spread in the estimated temperature spectra in our final uncertainty estimate. Uncertainties associated with the mean of the regional spectral estimates are computed assuming 10 spatial degrees of freedom [Jones et al., 1997], except for those associated with measurement changes, which are treated as systematic across records.

Available ensemble members associated with each model range from 1 to 23. In order to achieve uniform model weighting when calculating multimodel means, spectral analysis results associated with each ensemble member are inversely weighted according to the total number of ensemble members. This gives equal weighting across models, which is appropriate because ensemble members are generally tightly clustered relative to intermodel spread. Note that the spread of the ensemble provides a description of the CMIP5 collection but is only a lower bound on total model uncertainty [Knutti et al., 2010]. The results that we present from our analysis are robust to using either nearest neighbor or linear interpolation techniques, various

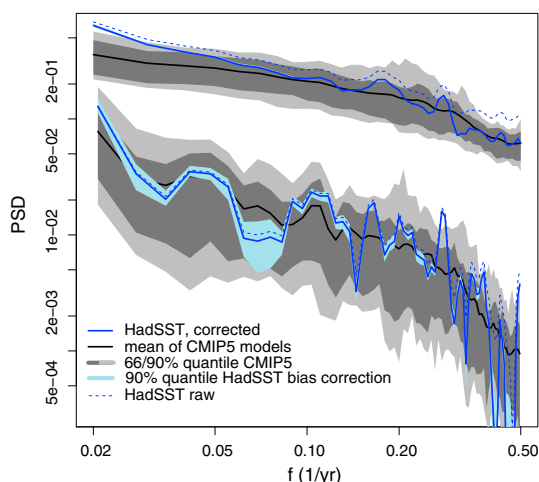


Figure 1. Regional versus global SST variability. At top is the average of local spectral estimates from instrumental observations and model simulations, and at bottom are the spectra estimated of global mean SST. Also shown are the 66% and 90% quantiles of the models (light and dark grey) and the 90% quantiles of the different realizations of the bias-corrected instrumental SSTs (light blue). Correction for the excess variance in SST observations caused by sampling and measurement error (dashed blue line versus blue line) has the strongest relative effect at interannual timescales.

frequencies, as also reported elsewhere [Solomon *et al.*, 2007; Crowley, 2000; Jones *et al.*, 2013], excepting near the frequencies associated with the El Niño–Southern Oscillation between 1/2 and 1/7 year, which is more strongly expressed in the observations than in most simulations. The mean of the regional spectra agrees at once per decade and higher frequencies, but at lower frequencies the observations show significantly greater spectral energy. Agreement for global average spectral estimates but disagreement at the regional level demonstrates that model temperature variability has, on average, greater positive spatial covariance than the observations at decadal timescales.

More insight into the mismatch between models and data can be gained from considering the ratio of spectral energies as a function of space (Figure 2). At interannual timescales, between 1/2 and 1/5 year⁻¹, the data-model ratio of spectral energy is near 1 when taking the zonal mean at most latitudes. Regionally, it is around 0.5 in the Northern North Atlantic, Northwestern Pacific, and Northern Indian Ocean, and 1.5 in the remainder of the Atlantic and Eastern Pacific (Table 1).

The data-model ratio at decadal timescales, between 1/20 and 1/50 years⁻¹, is larger than at interannual timescales (Figures 2 and 3). At middle and higher latitudes ($\geq 30^\circ$) the average data-model ratio is 1.3, with portions of the North Atlantic and Northwestern Pacific showing values less than 1 in a pattern similar to that seen at interannual timescales. At lower latitudes ($\leq 30^\circ$) the data-model ratio is 1.9, with only 4 out of 163 ensemble members showing greater variability than the observations: 2 of 10 ensemble members from the GFDL-CM2 model and 2 of 10 members from the HADCM3 model. It is also worth emphasizing that the correction for instrumental noise sources reduces the data-model ratio by as much as 100% at interannual timescales but by less than 30% at decadal timescales (Table 1). Temperature variations are of larger amplitude toward lower frequencies and are associated with a greater signal-to-noise ratio and are, therefore, less sensitive to noise correction. The noise correction would have to be more than a factor of 3 too small at decadal timescales, while being unchanged at interannual timescales, for the data and simulations to be consistent.

Our results thus confirm and update foregoing indications that regional model variability is weak relative to the observations at low latitudes and at decadal timescales [Stott and Tett, 1998; Davey *et al.*, 2002; DelSole, 2006]. It is also relevant to address the fact that other studies found general consistency when comparing the variability in average Eastern Tropical Pacific SSTs against the CMIP3 [Santer *et al.*, 2006] and CMIP5 [Fyfe and Gillett, 2014] model ensembles. These results can be understood in that averaging over the Eastern

filters to isolate variance at a particular timescale, and for the allowance of 2%, 10%, or 20% of missing data in choosing what records to include.

4. Model-Data Comparison

Spectral estimates associated with regional SST variability are much greater in magnitude than those associated with global average SST variability (Figure 1). The difference in variability is about 2 orders of magnitude at interannual timescales and decreases to less than an order of magnitude on multidecadal timescales. The global-regional differences reflect cancellation of variability in the global mean, and the weaker cancellation toward lower frequencies is consistent with findings that temperature anomalies have greater spatial autocorrelation toward longer timescales [Jones *et al.*, 1997].

For the global average, instrumental and model spectral estimates are generally consistent to within uncertainties across fre-

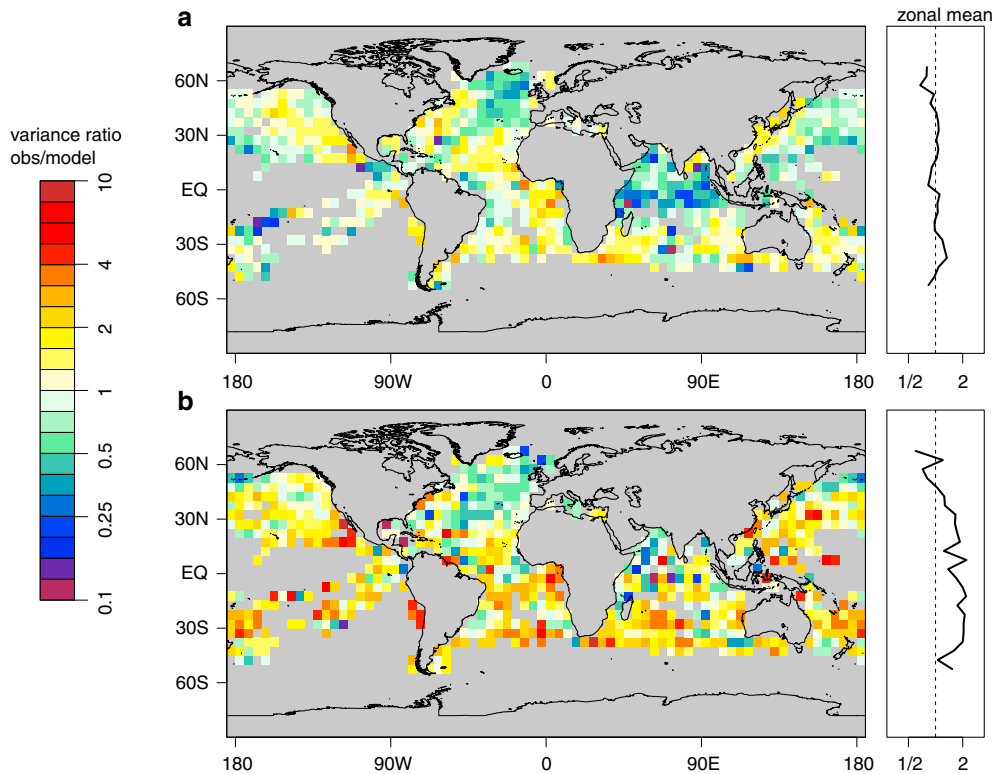


Figure 2. Variance ratio between the observed and simulated SSTs for (a) interannual (2–5 years) and (b) multidecadal (20–50) timescales. Simulated variance is the mean variance of all CMIP5 simulations. Observed variance is corrected for sampling and instrumental errors (see methods). Also shown is the zonal mean variance ratio between observed and simulated SSTs.

Equatorial Pacific reduces the apparent model-data inconsistency in the multidecadal band from a ratio of 2 to 1.6. This result follows from greater suppression of variability in the observations than in the models, consistent with our hypothesis of the models being too diffusive. Furthermore, analysis of average temperature produces a spread in variance ratios that is 24% larger than when the average is taken across the ratios computed for each grid box. Thus, analysis of average temperature reduces both discrepancies and detectability of discrepancies.

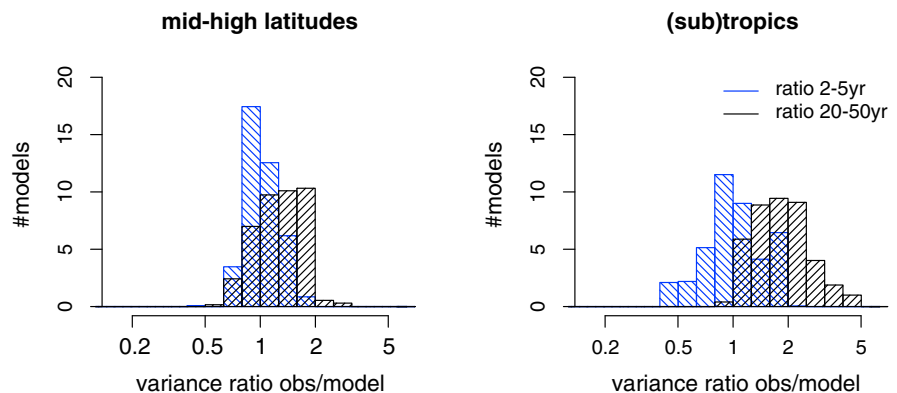


Figure 3. Distribution of the ratio between average instrumental and model SST variance for individual simulations. Shown are 2–5 year timescales (blue) and 20–50 year timescales (black) at middle to high latitudes (>30°N and >30°S) and low-latitude region (>30°S and <30°N).

5. Discussion and Conclusion

These results raise the question of why model simulations do not generate greater low-frequency SST variability at regional scales. It could be that models are too weakly forced at multidecadal timescales or contain insufficient positive feedback to amplify such forcing, but such a scenario seems unlikely to be a complete explanation because externally forced variability only accounts for a small fraction of regional model variance [Goosse *et al.*, 2005]. Comparing unforced simulations to an ensemble of forced simulations of the ECHAM5/MPIOM model [Jungclaus *et al.*, 2010] indicates that externally forced variability accounts for only 20% of the multidecadal tropical variability at $5 \times 5^\circ$ scales and even smaller fractions when including the extratropics. Assuming linearity, it can be inferred that doubling regional variability at $5 \times 5^\circ$ scales would require at least a fivefold increase in the externally forced contribution. Furthermore, interannual consistency at the regional level and across all timescales at the global level suggests that a marked increase in external variability would lead to other model-data mismatches.

More consistent with our findings is for the models to underestimate internal variability. The structure of the model-data mismatch suggests that model effective horizontal diffusivity may be too large, as this would lead to suppression of regional variability at low frequencies. Diffusivity would become important for the grid scale size that we analyze at approximately 8 years, where this timescale is derived from the square of the 500 km domain divided by an effective horizontal diffusivity of $1000 \text{ m}^2/\text{s}$. This timescale is consistent with the appearance of divergence between regional data and model spectra beginning in the vicinity of $1/8 \text{ years}^{-1}$ and increasing toward lower frequencies (Figure 1). Also of note is that Stammer [2005] showed that an initial specification of a uniform $1000 \text{ m}^2/\text{s}$ horizontal diffusivity in the MIT-GCM was generally revised downward through a formal data-fitting procedure.

Further insight can be gained by separating the multimodel ensemble according to resolution. Models are grouped into quartiles according to horizontal ocean resolution at the equator, and results are consistent with the diffusion hypothesis in the sense that lower resolution quartiles show less variability and a larger discrepancy with the observations. The lowest-resolution quartile of models has an average ratio of observed versus model variability of 2.8 in the tropics and 2.2 globally, whereas the highest-resolution quartile has analogous ratios of 1.7 and 1.4. Resolution is at best only a partial determinant of variability, however, as indicated by a 0.2 cross correlation between resolution and multidecadal variability across models.

Recent trends in global average temperature largely fall below those simulated by general circulation models [Fyfe *et al.*, 2013], and observed trends in Eastern Equatorial Pacific (EEP) SSTs are even more anomalously low relative to the models [Fyfe and Gillett, 2014]. These trends in EEP and global temperature appear related [Rahmstorf *et al.*, 2012; Kosaka and Xie, 2013; Fyfe *et al.*, 2013; Fyfe and Gillett, 2014]. We speculate that some of the model-data trend difference comes from simulations having too small internal variability. Greater internal variability in the models would widen the spread in the ensemble of model temperature trends and increase the likelihood of including the observed trend, especially if the greater variability is in regions having strong global teleconnections, such as in the EEP. Note that our result of greater actual SST variability is largely independent of the interval in question because all records span at least 100 years and end by 2005.

Although our results agree with earlier studies and are stable with respect to the time interval considered and various correction choices, there is some complication inherent to inferring variability during an interval containing substantial trends in global temperature. Spectral estimation and filtering assume quasi-stationarity over the interval of the record that cannot be entirely ensured through detrending. Distinguishing natural variability from forced variations that project onto natural modes of variability is also difficult. The use of paleodata to extend model-data comparisons and to include intervals prior to this last century seems a logical next step. Inasmuch as the hypothesis that excessive horizontal diffusion damps regional model variability holds, we expect even greater data-model discrepancies in variability toward lower frequencies.

References

- Bloomfield, P. (1976), *Fourier Decomposition of Time Series: An Introduction*, John Wiley, New York.
- Brohan, P., J. J. Kennedy, I. Harris, S. F. B. Tett, and P. D. Jones (2006), Uncertainty estimates in regional and global observed temperature changes: A new data set from 1850, *J. Geophys. Res.*, *111*, D12106, doi:10.1029/2005JD006548.
- Collins, M., S. F. B. Tett, and C. Cooper (2001), The internal climate variability of HadCM3, a version of the Hadley Centre coupled model without flux adjustments, *Clim. Dyn.*, *17*(1), 61–81.

Acknowledgments

The Program for Climate Model Diagnosis and Intercomparison and the World Climate Research Programme Working Group on Coupled Modeling made the WCRP CMIP5 simulations available. R. Ferrari, B. Fox-Kemper, and M. Miller provided helpful suggestions with regard to model diffusivity. C. Wunsch with regard to the manuscript and J. Kennedy with regard to the SST data. We thank the two anonymous reviewers for their constructive comments. T.L. was supported by the Initiative and Networking Fund of the Helmholtz Association, the Alexander von Humboldt Foundation and the Daimler and Benz foundation. P.H. acknowledges NSF grant 1304309.

The Editor thanks two anonymous reviewers for their assistance in evaluating this paper.

- Crowley, T. J. (2000), Causes of climate change over the past 1000 years, *Science*, 289(5477), 270–277, doi:10.1126/science.289.5477.270.
- Davey, M., et al. (2002), STOIC: A study of coupled model climatology and variability in tropical ocean regions, *Clim. Dyn.*, 18(5), 403–420, doi:10.1007/s00382-001-0188-6.
- DelSole, T. (2006), Low-frequency variations of surface temperature in observations and simulations, *J. Clim.*, 19(18), 4487–4507.
- Fyfe, J. C., and N. P. Gillett (2014), Recent observed and simulated warming, *Nat. Clim. Change*, 4(3), 150–151, doi:10.1038/nclimate2111.
- Fyfe, J. C., N. P. Gillett, and F. W. Zwiers (2013), Overestimated global warming over the past 20 years, *Nat. Clim. Change*, 3(9), 767–769.
- Goosse, H., H. Renssen, A. Timmermann, and R. S. Bradley (2005), Internal and forced climate variability during the last millennium: A model-data comparison using ensemble simulations, *Quat. Sci. Rev.*, 24(12–13), 1345–1360.
- Jones, G. S., P. A. Stott, and N. Christidis (2013), Attribution of observed historical near-surface temperature variations to anthropogenic and natural causes using CMIP5 simulations, *J. Geophys. Res. Atmos.*, 118, 4001–4024, doi:10.1002/jgrd.50239.
- Jones, P. D., T. J. Osborn, and K. R. Briffa (1997), Estimating sampling errors in large-scale temperature averages, *J. Clim.*, 10(10), 2548–2568.
- Jungclauss, J. H., et al. (2010), Climate and carbon-cycle variability over the last millennium, *Clim. Past*, 6(5), 723–737.
- Kennedy, J. J., N. A. Rayner, R. O. Smith, D. E. Parker, and M. Saunby (2011a), Reassessing biases and other uncertainties in sea surface temperature observations measured in situ since 1850: 1. Measurement and sampling uncertainties, *J. Geophys. Res.*, 116, D14103, doi:10.1029/2010JD015218.
- Kennedy, J. J., N. A. Rayner, R. O. Smith, D. E. Parker, and M. Saunby (2011b), Reassessing biases and other uncertainties in sea surface temperature observations measured in situ since 1850: 2. Biases and homogenization, *J. Geophys. Res.*, 116, D14104, doi:10.1029/2010JD015220.
- Knutti, R., R. Furrer, C. Tebaldi, J. Cermak, and G. A. Meehl (2010), Challenges in combining projections from multiple climate models, *J. Clim.*, 23(10), 2739–2758.
- Kosaka, Y., and S.-P. Xie (2013), Recent global-warming hiatus tied to equatorial Pacific surface cooling, *Nature*, 501(7467), 403–407, doi:10.1038/nature12534.
- Laepple, T., and P. Huybers (2013), Reconciling discrepancies between Uk37 and Mg/Ca reconstructions of Holocene marine temperature variability, *Earth Planet. Sci. Lett.*, 375, 418–429, doi:10.1016/j.epsl.2013.06.006.
- McCoy, E., A. Walden, and D. Percival (1998), Multitaper spectral estimation of power law processes, *IEEE Trans. Signal Process.*, 46(3), 655–668.
- Min, S. K., S. Legutke, A. Hense, and W. T. Kwon (2005), Internal variability in a 1000-yr control simulation with the coupled climate model ECHO-G I. Near-surface temperature, precipitation and mean sea level pressure, *Tellus Ser. A*, 57, 605–621.
- Percival, D. B., and A. T. Walden (1993), *Spectral Analysis for Physical Applications: Multitaper and Conventional Univariate Techniques*, Cambridge Univ. Press, Cambridge, U. K.
- Rahmstorf, S., G. Foster, and A. Cazenave (2012), Comparing climate projections to observations up to 2011, *Environ. Res. Lett.*, 7(4), 044035, doi:10.1088/1748-9326/7/4/044035.
- Rhines, A., and P. Huybers (2011), Estimation of spectral power laws in time uncertain series of data with application to the Greenland Ice Sheet Project 2 $\delta^{18}\text{O}$ record, *J. Geophys. Res.*, 116, D01103, doi:10.1029/2010JD014764.
- Santer, B. D., et al. (2006), Forced and unforced ocean temperature changes in Atlantic and Pacific tropical cyclogenesis regions, *Proc. Nat. Acad. Sci.*, 103(38), 13,905–13,910, doi:10.1073/pnas.0602861103.
- Solomon, S., D. Qin, M. Manning, Z. Chen, M. Marquis, K. B. Averyt, M. Tignor, and H. L. Miller (2007), *Climate Change 2007—The Physical Science Basis: Working Group I Contribution to the Fourth Assessment Report of the IPCC*, Cambridge Univ. Press, Cambridge, U. K., and New York.
- Stammer, D. (2005), Adjusting internal model errors through ocean state estimation, *J. Phys. Oceanogr.*, 35(6), 1143–1153.
- Stott, P. A., and S. F. B. Tett (1998), Scale-dependent detection of climate change, *J. Clim.*, 11(12), 3282–3294.
- Taylor, K. E., R. J. Stouffer, and G. A. Meehl (2012), An overview of CMIP5 and the experiment design, *Bull. Am. Meteorol. Soc.*, 93(4), 485–498, doi:10.1175/BAMS-D-11-00094.1.
- Wilson, P. S., A. C. Tomsett, and R. Toumi (2003), Long-memory analysis of time series with missing values, *Phys. Rev. E*, 68(1), 017103, doi:10.1103/PhysRevE.68.017103.